Organic cation transport in the rat kidney *in vivo* visualized by time-resolved two-photon microscopy

M Hörbelt[1,2], C Wotzlaw[2], TA Sutton[3], BA Molitoris[3], T Philipp[1], A Kribben[1], J Fandrey[2] and F Pietruck[1]

[1]Department of Nephrology, School of Medicine, University Hospital, Essen, Germany; [2]Institute of Physiology, School of Medicine, University Hospital, Essen, Germany and [3]Division of Nephrology, Department of Medicine and the Indiana Center for Biological Microscopy, Indiana University School of Medicine, Indianapolis, Indiana, USA

Secretion of cationic drugs and endogenous metabolites is a major function of the kidney accomplished by tubular organic cation transport systems. A cationic styryl dye (ASP^+) was developed as a fluorescent substrate for renal organic cation transporters. The dye was injected intravenously and continuously monitored in externalized rat kidneys by time-resolved two-photon laser scanning microscopy. To investigate changes in transport activity, cimetidine, a competitive inhibitor of organic cation transport was co-injected with ASP^+. Shortly after injection, fluorescence increased in peritubular capillaries. Simultaneously, fluorescence was transiently found at the basolateral membrane of the proximal and distal tubules at a higher intensity and shorter wavelength indicating membrane association of ASP^+. Subsequently, intracellular fluorescence increased steeply within 10 s. In the proximal tubules, intracellular fluorescence decreased by 50% within 5 min, while in the distal tubules the fluorescence decreased by only 5% within the same time frame. Intracellular uptake of ASP^+ into proximal tubules was significantly reduced by cimetidine. Our studies show that organic cation transport of the kidney can be visualized *in vivo* by two-photon laser scanning microscopy.

One major function of the kidney is the elimination of organic compounds including drugs or endogenous substances from the body. This is accomplished by net secretion of the respective substances by proximal tubules. According to their physicochemical properties, secreted substances can be classified either as organic anions or as organic cations (OC). Many clinically used drugs including β-blockers, calcium antagonists, antibiotics, hypoglycemic agents, diuretics, and morphine analogs, as well as endogenous substances including catecholamines and neurotransmitters are OC.

Tubular secretion of OC is accomplished by polyspecific OC transporters of the solute carrier drug transporter family 22 (SLC 22). These transporters are located in the plasma membranes of proximal tubules. Transport involves tubular uptake of OC from the blood across basolateral membranes and tubular secretion into the tubule lumen across apical membranes.[1–3]

Investigations of OC transport have been performed mainly by using radiolabeled substrates like tetraethylammonium$^+$, N^1-methylnicotinamide$^+$, or N-methyl-4-phenylpyridinium$^+$. However, the number of measurements of the transported substances is limited by the time interval necessary for the collection of samples.[4–6] The resulting poor temporal resolution prevents continuous observations of transport processes and reduces measurements to distinct time points. Furthermore, the methods used so far, do not give much information about the intracellular distribution and behavior of the tested OC.

Fluorescent substrates may serve as advantageous probes because they allow continuous measurements in real time.[7,8] We identified the cationic styryl dye (4-(4-dimethylamino)-styryl)-N-methylpyridinium (ASP^+) as a fluorescent substrate of renal organic cation transporters.[9] Later, Stachon *et al.*[10] confirmed the value of ASP^+ for OC transport measurements in LLC-PK_1 cells. Additionally, ASP^+ was used for OC transport studies in other cell culture models[11–13] and in isolated proximal tubules.[14,15]

Various experimental models have previously been applied for studies of OC transport including cellular substructures,[16,17] cell expression systems,[5] and cultured cells.[18,19] However, these experimental models possess particular limitations. In order to survive *in vitro*, cultured cells

undergo a variety of adaptive phenotypic changes. This is particularly problematic for proximal tubule cells because they change under culture conditions from their physiological dependence on oxidative metabolism to glycolysis.[20] In contrast, freshly isolated proximal tubules retain a high degree of structural integrity as well as biochemical and functional properties of the *in vivo* state and they represent a good model to exclude vascular or hormonal effects.[15,21] Structural and functional properties may even be better retained in the context of the surrounding tissue using the model of *in situ* perfusion of individual tubules and their associated capillaries in living animals.[22,23] However, *in vivo* studies of intact kidneys most likely approach original renal physiology, since the context of the whole organism is retained.

In 2002, Dunn *et al.*[24] introduced the method of intravital two-photon laser scanning microscopy (2P-LSM) of the rat kidney. Since then, this real-time imaging technique has opened up new fields for functional investigations in kidneys of living animals using endogenous or exogenous fluorescent dyes.[25–28] 2P-LSM is a valuable tool to study biological actions in the kidney, because due to non-invasive deep tissue penetration, the original microenvironment of the organ remains preserved.[29]

The aim of this study was to develop a method to visualize OC transport in the intact rat kidney *in vivo*, using ASP^+ and 2P-LSM. Furthermore, we tested whether alterations of OC transport can be detected with this method.

RESULTS

Intravital imaging of tubular ASP^+ uptake in the rat kidney

Tubular ASP^+ uptake was observed *in vivo* and occurred rapidly after intravenous injection as can be seen in Figure 1, presenting short-term changes of kidney fluorescence during ASP^+ transport. Before ASP^+ injection, proximal tubule segments exhibited significant autofluorescence, whereas autofluorescence of distal tubules was negligible. From 5 to 15 s after ASP^+ injection, a transient increase in fluorescence was observed in peritubular capillaries and in the peritubular space. Nuclei of endothelial cells as well as red blood cells were indirectly visible as non-fluorescent shadows. This was paralleled by a transient and pronounced fluorescence of adjacent plasma membranes including the basolateral membranes of tubular cells. At basolateral membranes, ASP^+ fluorescence appeared green, indicating a shift to shorter wavelengths (blue-shift), which suggests binding of
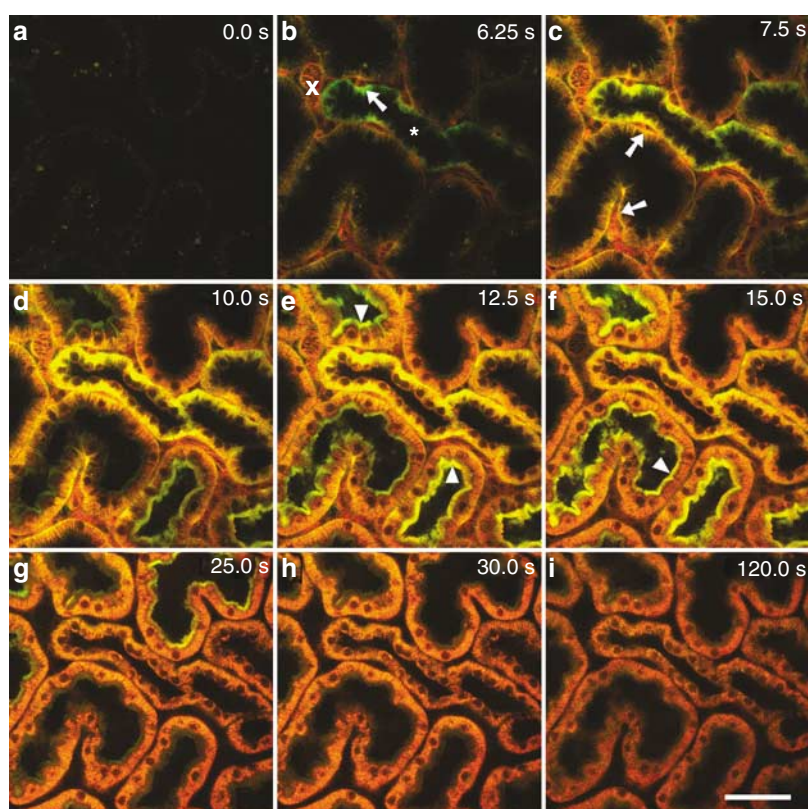

Figure 1 | Short-term distribution of fluorescence in the kidney after ASP^+ injection. A 0.2 ml bolus containing 0.3 μmol ASP^+ (1.5 mM final concentration) was injected intravenously and kidney fluorescence was continuously monitored by 2P-LSM. (**a**) Before injection, only autofluorescence was observed in proximal tubule segments. (**b** and **c**) After ASP^+ injection, fluorescence appeared in peritubular capillaries omitting red blood cells (×). In parallel, fluorescence appeared outside the capillaries and a transient, pronounced, and blue-shifted fluorescence was observed at basolateral membranes (arrows). Subsequently, intracellular fluorescence rapidly increased in proximal and distal (asterisk) tubules starting from the basolateral side, omitting the nuclei. (**d–f**) A transient and pronounced fluorescence was observed at the brush-border membranes of proximal tubules where it was shifted to shorter wavelengths (arrowheads). (**g–i**) Intracellular fluorescence decreased slowly over time. The length of the sizing bar corresponds to 50 μm.

ASP$^+$ to the outer lipid layer of plasma membranes.[30] Subsequently, a rapid increase of intracellular fluorescence occurred in all proximal and distal tubules that started from the basolateral side, omitted the nuclei, and was maximal 10 s after the first appearance of ASP$^+$ in peritubular capillaries. In earlier segments of proximal tubules, brush-border membranes showed transient and pronounced fluorescence, but this was not observed in later proximal segments (for determination of earlier and later proximal segments see Figures 4 and 5). The observed fluorescence at the brush-border membranes was blue-shifted, similar to the observation at basolateral membranes. Furthermore, the luminal fluid of proximal as well as of distal tubules did not show significant ASP$^+$ fluorescence. Once fluorescence had disappeared from the peritubular space, intracellular fluorescence started to decrease slowly over time.

Time course of tubular ASP$^+$ fluorescence in the rat kidney

A decrease of ASP$^+$ fluorescence was observed in proximal tubules within 40 min after intravenous injection as can be seen in Figure 2, presenting long-term changes of kidney
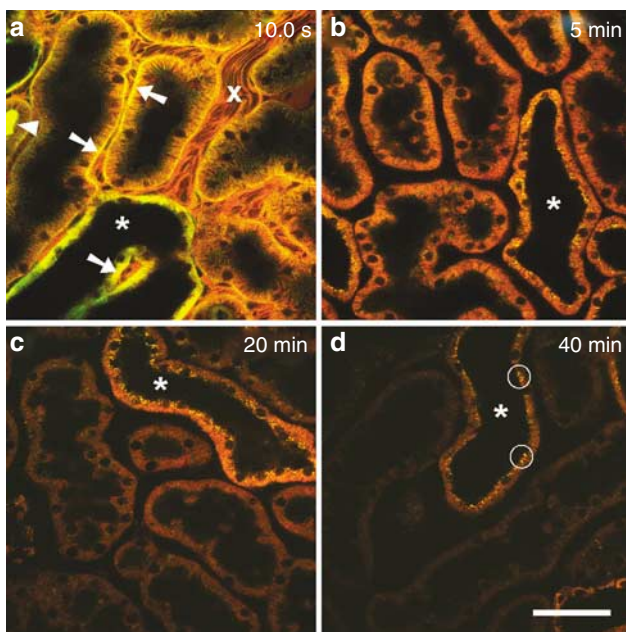
Figure 2 | Prolonged distribution of fluorescence in the kidney after ASP$^+$ injection. A 0.2 ml bolus containing 0.3 μmol ASP$^+$ (1.5 mM final concentration) was injected intravenously. Subsequently, ASP$^+$ distribution in the kidney cortex was monitored over 40 min by 2P-LSM. (**a**) Capillary fluorescence omitted red blood cells ($\times$). Transient and pronounced fluorescence was observed at basolateral (arrows) and at brush-border membranes (arrowhead) where it was shifted to shorter wavelengths. Intracellular fluorescence in proximal and distal (asterisk) tubules omitted the nuclei. (**b–d**) Intracellular fluorescence of proximal tubule segments decreased to baseline within 40 min. During this time, intracellular fluorescence in distal tubules (asterisks) was largely preserved and was partially translocated into subcellular vesicles at the apical aspect of these cells (circles). The length of the sizing bar corresponds to 50 μm.

fluorescence during ASP$^+$ transport. In proximal tubules, intracellular fluorescence decreased to baseline within 40 min after ASP$^+$ injection. In distal tubules, intracellular fluorescence was largely preserved over 40 min with a translocation of ASP$^+$ into subcellular vesicles predominantly located in the apical part of these cells. Additionally, quantitative image analysis of intracellular fluorescence revealed that maximal fluorescence in proximal tubules was decreased by 50% after 5 min, whereas in distal tubules intracellular fluorescence was only decreased by 5% after 5 min.

Quantification of ASP$^+$ transport and its inhibition by cimetidine

The inhibitor of OC transport, cimetidine, significantly inhibited ASP$^+$ transport in proximal tubules. After ASP$^+$ injection, quantitative analysis of intracellular fluorescence in proximal tubules revealed a steep rise in intensity for 10 s followed by a slow but continuous decrease in ASP$^+$ fluorescence intensity (Figure 3). Co-injection of cimetidine together with ASP$^+$ resulted in significantly lower maximal intracellular fluorescence intensity and a slower time-dependent decrease in fluorescence, regardless whether it was injected before or after ASP$^+$ control injection (Figure 3). Integrated ASP$^+$ fluorescence intensities were reduced by $41.8 \pm 3.3\%$ (21.8 ± 2.4 integrated units in control rats vs 12.6 ± 1.5 integrated units in the presence of cimetidine; $P < 0.01$, $n = 5$; data not shown).

The contribution of filtered ASP$^+$ to the observed fluorescence

The transient brush-border fluorescence was associated with glomerularly filtered ASP$^+$. After simultaneous injection of ASP$^+$ together with a small molecular weight dextran (Texas Red labeled), combined fluorescence of both injected dyes was temporarily observed in the peritubular space during the passage of the injected bolus, whereas fluorescence of basolateral membranes and intracellular compartments was similar to that of ASP$^+$ alone. Transient luminal fluorescence was observed in the presence of labeled dextran in all proximal segments at different time points (Figure 4) with a fluorescence spectrum of the luminal fluid being in accordance to that of Texas Red labeled dextran. The time between injection and first appearance of luminal dextran fluorescence was regarded as filtrate passage time. In earlier proximal tubular segments with a shorter filtrate passage time, luminal dextran fluorescence coincided with a transient and pronounced ASP$^+$ fluorescence of the brush-border membrane. In later proximal tubule segments with a longer filtrate passage time, brush-border fluorescence was not observed at all.

Correlation of brush-border fluorescence with filtrate passage time

Brush-border fluorescence decreased during the passage of ASP$^+$ along proximal tubules. The filtrate passage time in proximal tubule segments varied from 5 to 60 s in all observed
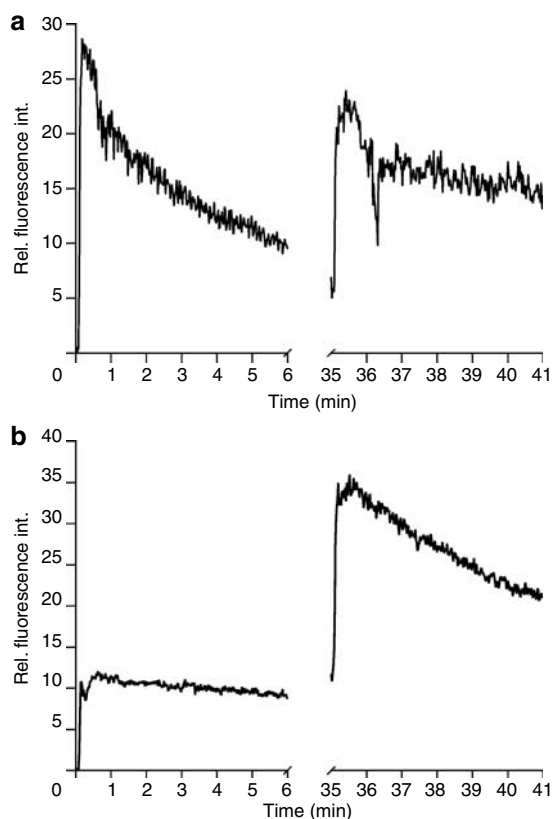
Figure 3 | Effect of cimetidine on tubular ASP⁺ transport.
Fluorescence intensity of proximal tubules, continuously recorded by
2P-LSM after injection of ASP⁺ only and ASP⁺ together with
cimetidine. Depicted are two typical experiments. (**a**) In the first
experiment, an ASP⁺ control injection was followed by an injection
of ASP⁺ plus cimetidine. (**b**) In the second experiment, the first
injection contained ASP⁺ together with cimetidine and was followed
by a control injection containing ASP⁺ alone. Each 0.2 ml injection
bolus contained either 0.3 μmoles ASP⁺ alone (1.5 mM final
concentration) or 0.3 μmoles ASP⁺ plus 8 μmoles cimetidine (40 mM
final concentration), respectively. The second injection was started
35 min after the first injection as indicated.

proximal tubular segments. Figure 5 shows that maximal brush-
border membrane fluorescence intensity in proximal tubule
segments inversely correlates with filtrate passage time. Intracel-
lular fluorescence intensity increased simultaneously in all
proximal tubule segments, but maximal intensity was highest
in earlier segments with short filtrate passage time.

DISCUSSION

In this study we demonstrate for the first time that 2P-LSM
together with the fluorescent substrate ASP⁺ can be applied
in vivo for continuous monitoring of OC transport in the
kidney.

Thereby OC transport occurs from the peritubular
capillaries across the basolateral membrane toward the
tubular lumen. ASP⁺ uptake was observed not only in
proximal but also in distal tubules.

Before ASP⁺ passes the basolateral membrane, transient
shifts of fluorescence to shorter wavelengths (blue-shift)

could be noticed at plasma membranes of endothelial as well
as tubule cells. This blue-shift of fluorescence depends on the
temporary localization of ASP⁺ molecules in the outer lipid
layer of the plasma membrane. Significant blue-shifts are
caused by interaction of the dye molecules with the strong
intra-membrane dipole potential, based on electrochromism
(Stark effect).[30,31]

As we used a bolus injection of ASP⁺, the extent of net
ASP⁺ uptake into tubules was limited due to transient
delivery of ASP⁺ by peritubular capillaries. Nevertheless,
ASP⁺ uptake appeared to be highly effective, which is
consistent with earlier in vitro reports.[10,14,15]

However, we observed differences in the way intracellular
ASP⁺ fluorescence decreased in proximal and distal tubules.
In proximal tubules, intracellular ASP⁺ fluorescence de-
creased over time. Previous studies revealed that transport of
OC across the apical membrane of proximal tubules is
relatively slow and is probably the rate-limiting step of OC
secretion.[6,32] In contrast, Dantzler et al.[33] measured high OC
efflux rates in isolated brush-border membrane vesicles which
indicates that pharmacokinetic properties of apical transpor-
ters might not be responsible for delayed OC secretion. These
authors hypothesized that substrate availability at the apical
membrane might be reduced due to intracellular binding or
sequestration of OC. Furthermore, net reabsorption of OC
along the nephron was observed in earlier studies and could
contribute to tubular retention of ASP⁺.[9,34]

Distal tubular uptake of OC has been described in the
literature using radiolabeled substrates.[35,36] In our studies of
distal tubules in vivo, the majority of intracellular ASP⁺ was
retained during the observation time of a single injection and
further on during the whole experimental period of up to
3–4 h. Moreover, ASP⁺ was translocated into subcellular
vesicular compartments, which were exclusively observed in
the distal nephron. Pritchard et al.[37] reported the presence of
OC exchange systems in membranes of acidifying endosomes
isolated from rat renal cortex, but the origin of the isolated
endosomes, whether proximal or distal, was not determined.

Furthermore, in most proximal tubule segments, ASP⁺
fluorescence was observed at the brush-border membrane,
but fluorescence was never observed in the tubular lumen
although a significant amount of ASP⁺ is filtered by
glomeruli.[9] The reason for this discrepancy may be that the
fluorescence quantum yield of styryl dyes increases by orders
of magnitude in the presence of biological macromolecules
compared to aqueous solutions.[38,39] In analogy, the high
fluorescence intensity of ASP⁺ in peritubular capillaries may
be caused by the presence of plasma proteins.

In order to examine a possible coincidence of the brush-
border ASP⁺ fluorescence and the luminal passage of ASP⁺
originating from the injected bolus, we co-injected fluor-
escent dextran of low molecular weight of neutral charge,
which is freely filtered by glomeruli, together with ASP⁺,
visually indicating the time of luminal filtrate passage. Our
observations of luminal dextran fluorescence revealed that
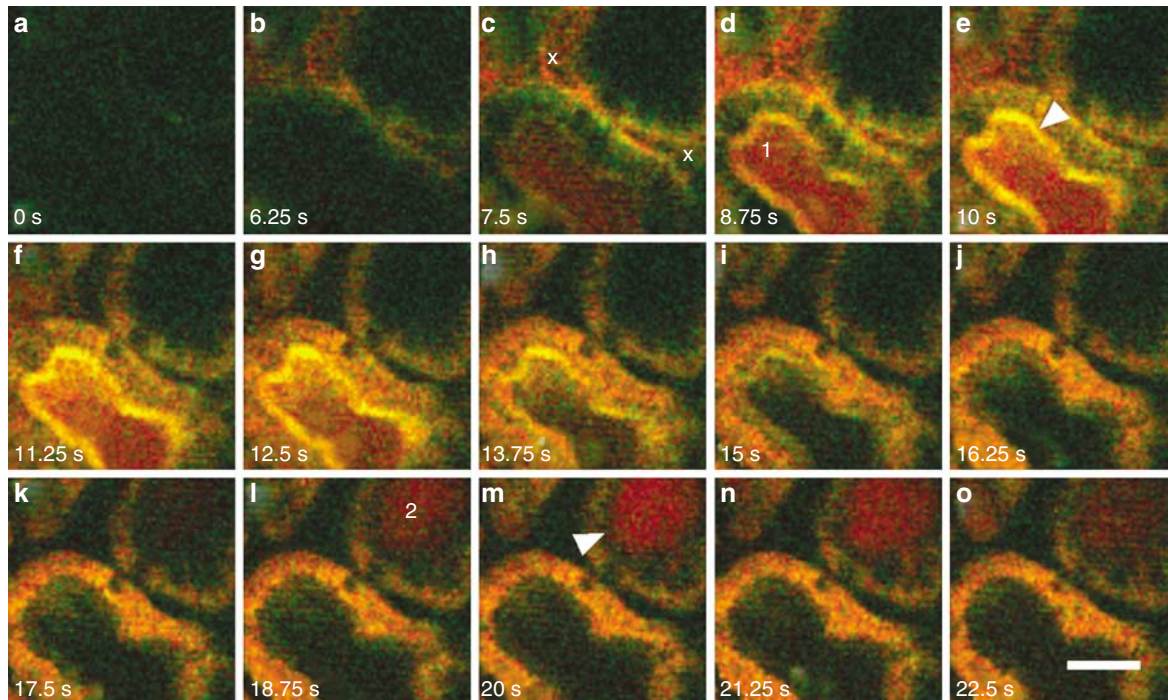obviously luminal ASP⁺ had caused the blue-shifted

Figure 4 | Changes of fluorescence caused by the filtered ASP⁺ fraction. A low molecular weight fluorescent dextran (3 kDa) labeled with Texas Red was utilized to visualize the luminal passage of the glomerulus filtrate. ASP⁺ and dextran were co-injected into the jugular vein and fluorescence of the kidney cortex was continuously monitored by 2P-LSM. (**a–c**) Shortly after injection, fluorescence increased in the peritubular capillaries (×). (**c–j**) In an early proximal tubule segment (**d**, 1), transient luminal red fluorescence, supposedly originating from filtered Texas Red, occurred 7.5 s after injection. This was paralleled by a transient and pronounced green–yellow fluorescence at the brush border originating from filtered ASP⁺ (arrowhead in **e**). (**k–o**) In a late proximal tubule segment (**l**, 2), the transient luminal fluorescence of Texas Red occurred 18.75 s after injection. This was not paralleled by brush-border fluorescence (arrowhead in **m**). The tubule segment with early luminal fluorescence and intense brush-border fluorescence subsequently exhibited higher intracellular fluorescence than the tubule segment with late luminal fluorescence (**o**). The length of the sizing bar corresponds to 25 μm.

fluorescence of adjacent brush-border membranes during its luminal passage. ASP⁺ fluorescence of the brush-border membrane continuously decreased with the distance of proximal tubule segments to the glomerulus. One reason for this may be that tubular reabsorption of ASP⁺ occurs during its passage through the nephron.[9]

Another objective of this study was to test, if alterations of tubular ASP⁺ transport could be detected by 2P-LSM. Therefore, ASP⁺ transport was competitively inhibited by the organic cation cimetidine. Our experiments revealed a 42% reduction of proximal tubule ASP⁺ uptake in the presence of cimetidine, which is consistent with *in vitro* data.[19] Furthermore, after uptake into the intracellular compartment, time-dependent decreases of intracellular ASP⁺ in proximal tubules were less in the presence of cimetidine. This may be due to several reasons. Reduced intracellular dye load may decrease the transmembrane dye gradient resulting in reduced outward driving force and reduced secretory activity. Likewise, cimetidine taken up across the basolateral membrane may compete with ASP⁺ for luminal secretion, resulting in a competitive inhibition of ASP⁺ secretion. Even trans-stimulation of luminal ASP⁺ reabsorption by cimetidine may result in decreased net secretion of ASP⁺.[9]

In conclusion, we have demonstrated for the first time that OC transport can be studied continuously in the rat kidney *in vivo* using 2P-LSM and the fluorescent substrate ASP⁺. ASP⁺ can be visualized simultaneously in the microvasculature, proximal, and distal tubules with a high spatial resolution.

MATERIALS AND METHODS
Animals
In Indianapolis (IN, USA), male Sprague–Dawley rats (Harlan, Indianapolis, IN, USA) weighing 200–300 g were used as described below. All experiments were conducted in accordance with the *Guide for the Care and Use of Laboratory Animals* (Washington, DC: National Academy Press, 1996) and were approved by the *Institutional Animal Care and Use Committee*. In Essen, Germany, male Sprague–Dawley rats (Charles River, Sulzfeld, Germany) weighing 200–300 g were used. All experiments were conducted in accordance with the *German Laboratory Animal Protection Law* (§ 8 Tierschutzgesetz, 1998; BGB I, S. 1105) and approved by the *Bezirksregierung Düsseldorf* (Aktenzeichen: 50.05-230-71/04; TSG-Nr. G 785/04).

Preparation of the left kidney for intravital imaging
The rats were anesthetized with an intraperitoneal injection of either pentobarbital sodium (65 mg/kg) (Indianapolis) or ketamine
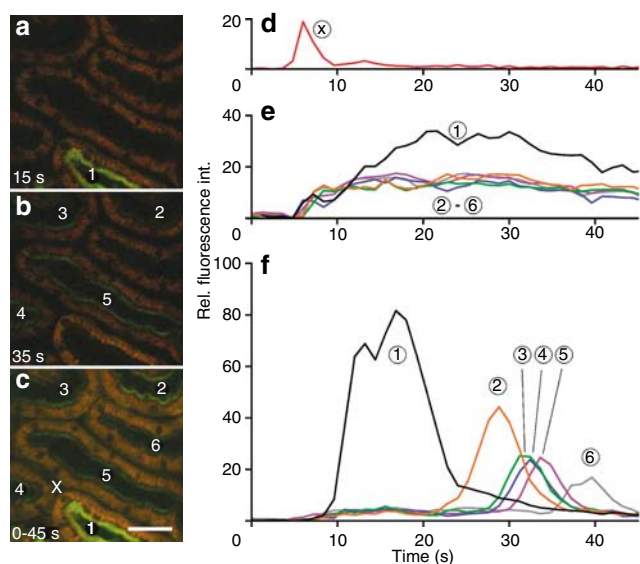
Figure 5 | Segmental differences of proximal tubule fluorescence as a function of time after ASP$^+$ injection. (a–c) ASP$^+$ was injected intravenously and fluorescence of the kidney cortex was continuously monitored with 2P-LSM. Images (**a** and **b**) display the ASP$^+$ fluorescence of proximal tubule segments at 15 and 35 s after injection, respectively. Panel c displays the maximal intensity determined for each pixel over 45 s as a composite image. In all proximal tubule segments in the area of view, a transient and pronounced ASP$^+$ fluorescence occurred at the brush-border region within 45 s, shifted to shorter wavelengths. The numbering (1–6) of the imaged tubule segments denotes the sequence of the transient brush-border fluorescence. The '×' denotes the lumen of a peritubular capillary. The sizing bar corresponds to a distance of 50 μm. (d–f) The graphs display fluorescence changes in a peritubular capillary (**d** '×'), in the intracellular part (**e**) and the brush-border regions (**f**) of different proximal tubule segments (1–6) over time. Numbering in graphs (**d–f**) corresponds to numbered tubule segments (**a–c**). Shortly after the capillary fluorescence (**d** '×'), intracellular fluorescence increased in all tubule segments (**e**). Brush-border fluorescence intensity inversely correlated with the time of appearance (**f**). The tubule segment with earliest and most intense brush-border fluorescence (**f** '①') subsequently exhibited a higher intracellular fluorescence (**e** '①') than other segments.

hydrochloride (100 mg/kg) plus xylazine hydrochloride (2 mg/kg) (Essen), respectively, and placed on a homeothermic table to maintain core body temperature at 37°C. A polyethylene catheter was inserted into the external jugular vein by microdissection for intravenous infusion and the left kidney was externalized through a flank incision without removal of the capsule. Thereafter, rats were placed on their left side onto the microscope stage. The externalized kidney rested in a glass bottom dish where it was kept moist in warmed 0.9% saline until the end of the experiment. On stage, the animals were covered with a temperature controlled circulating water-heating blanket (Gaymar Industries, Buffalo, NY, USA). Additionally, mean arterial blood pressure of the rats was monitored in the femoral artery using a BLPR/BP-1 blood pressure monitor (World Precision Instruments, Berlin, Germany) to assure that changes were <10% from the initial value throughout the time of the experiment. Finally, the animals were killed during anesthesia.[40]

Intravital 2P-LSM

Two-photon images of the kidney were scanned with a Bio-Rad MRC 1024 MP Laser Scanning Confocal/Multiphoton Scanner (Bio-Rad, Hercules, CA, USA), which was equipped with a Tsunami Lite titanium-sapphire laser (Spectra-Physics, Mountain View, CA, USA) tuned to a wavelength of 800 nm. The microscope stage was attached to a Nikon Diaphot inverted microscope (Fryer, Huntley, IL, USA) and was utilized to position the kidney in the glass bottom dish exactly above the objective as described.[24] Alternatively, two-photon images were captured with a Nikon Eclipse TE300 inverted microscope employing a Coherent Mira 900F titanium-sapphire laser (Coherent, Dieburg, Germany) tuned to a wavelength of 800 nm.[41] The focus of the optical image plane was set at 30 μm below the kidney surface, which was the best depth for a concurrent observation of tubule cells, tubule lumen, and the peritubular capillary network. The acquired images consisted of red and green color channels where 'red' was assigned to the photomultiplier that was preceded by a 605/90 nm band pass filter and 'green' was assigned to the photomultiplier that was preceded by a 525/50 nm band pass filter. For studies of time-resolved fluorescence dynamics, images were scanned at 160 × 160 resolution and 1.25 s per frame. For morphological studies, images were scanned at 512 × 512 resolution. All presented images have been amplified in pixel intensity for visibility of structures. Quantitative data were derived from original images without saturation of pixel intensities.

Live studies of organic cation transport in the rat kidney with ASP$^+$

Two-photon images of tubular autofluorescence were recorded in the absence of exogenous fluorescent organic cations. To detect dynamic changes of fluorescence intensity and distribution, the fluorescent organic cation 4-(4-(dimethylamino)styryl)-*N*-methyl-pyridinium (ASP$^+$) (Molecular Probes, Eugene, OR, USA) was applied by single bolus injection. For each experiment, 0.2 ml of warmed phosphate-buffered saline buffer at pH 7.4 containing 0.3 μmoles of ASP$^+$ (1.5 mM final concentration) were injected intravenously via the jugular catheter, and fluorescence in the kidney was recorded continuously for 5 min by time-resolved two-photon imaging. Subsequently, images were scanned randomly at various regions of the kidney cortex for up to 40 min after ASP$^+$ injection.

Live inhibition studies of ASP$^+$ transport with cimetidine

To investigate alterations of ASP$^+$ transport, cimetidine, a competitive inhibitor of OC transport,[19] was co-injected with ASP$^+$. For each experiment, 8 μmoles of cimetidine (Sigma, St Louis, MO, USA) were dissolved in 0.2 ml of warmed phosphate-buffered saline buffer at pH 7.4 (40 mM final concentration) also containing 0.3 μmoles of ASP$^+$ (1.5 mM final concentration) and injected into the jugular vein. Injections containing ASP$^+$ only or injections containing ASP$^+$ together with cimetidine were applied to the same animal with alternating order at 35 min time intervals. After injection, fluorescence in proximal tubules was continuously recorded as described above.

Quantitative measurement of ASP$^+$ fluorescence in the rat kidney

Quantitative analysis of the scanned fluorescence images was performed with ImageJ software (National Institutes of Health (http://rsb.info.nih.gov/ij/), Bethesda, MD, USA). Region of interest

analysis was utilized to determine fluorescence intensities of peritubular capillaries, intracellular compartments of proximal, and distal tubules as well as brush-border membranes and the tubule lumen. Fluorescence image series were scanned after ASP$^+$ injection and contained 4–6 imaged tubule segments. Fluorescence intensities before injection were regarded as baseline and were subtracted from all data before analysis. To determine the inhibitory effect of cimetidine on ASP$^+$ transport, intracellular fluorescence intensity was quantified in the presence or absence of cimetidine and was integrated over 60 s (referred to as integrated units) starting from the time of increase in fluorescence.

Contribution of filtered ASP$^+$ to the observed fluorescence

Due to low quantum yields of ASP$^+$ fluorescence in aqueous solutions, fluorescence of the luminal fluid was not observed in any of the tubules. To identify the time point of first luminal passage of filtered ASP$^+$, a fluorescent dextran of low molecular weight that is freely filtered by glomeruli was co-injected with ASP$^+$. Therefore, 1.3 mg dextran (3 kDa, Texas Red labeled, Molecular Probes) was added to a 0.2 ml bolus of warmed phosphate-buffered saline buffer at pH 7.4 containing 0.3 μmol ASP$^+$ (1.5 mM final concentration). Fluorescence in the kidney cortex was continuously recorded for 6 min after ASP$^+$ and dextran injection as described above. To further investigate segmental differences of the transient brush-border membrane fluorescence of proximal tubules, quantitative image analysis was performed in experiments where ASP$^+$ alone was injected. Fluorescence in proximal tubules was continuously recorded for 5 min after ASP$^+$ injection. For these images, the filtrate passage time was determined for each proximal tubular segment as the time between injection and first appearance of the transient brush-border membrane fluorescence and was compared with maximal ASP$^+$ fluorescence intensity of the brush border.

Statistical analysis

All data are means and were corrected for baseline levels. Comparison of integrated fluorescence intensities was carried out with Student's *t*-test and values are expressed as mean integrated units ± s.e. $P < 0.05$ were considered statistically significant.

REFERENCES
1. Koepsell H, Schmitt BM, Gorboulev V. Organic cation transporters. *Rev Physiol Biochem Pharmacol* 2003; **150**: 36–90 (E-pub 2003 June 25).
2. Ciarimboli G, Schlatter E. Regulation of organic cation transport. *Pflugers Arch* 2005; **449**: 423–441.
3. Wright SH. Role of organic cation transporters in the renal handling of therapeutic agents and xenobiotics. *Toxicol Appl Pharmacol* 2005; **204**: 309–319.
4. Sokol PP, McKinney TD. Mechanism of organic cation transport in rabbit renal basolateral membrane vesicles. *Am J Physiol* 1990; **258**: F1599–F1607.
5. Busch AE, Quester S, Ulzheimer JC *et al*. Electrogenic properties and substrate specificity of the polyspecific rat cation transporter rOCT1. *J Biol Chem* 1996; **271**: 32599–32604.
6. Jonker JW, Wagenaar E, Van Eijl S *et al*. Deficiency in the organic cation transporters 1 and 2 (Oct1/Oct2 [Slc22a1/Slc22a2]) in mice abolishes renal secretion of organic cations. *Mol Cell Biol* 2003; **23**: 7902–7908.
7. Ammer U, Natochin Y, Ullrich KJ. Tissue concentration and urinary excretion pattern of sulfofluorescein by the rat kidney. *J Am Soc Nephrol* 1993; **3**: 1474–1487.
8. Steinhausen M, Muller P, Parekh N. Renal test dyes IV. Intravital fluorescence microscopy and microphotometry of the tubularly secreted dye sulfonefluorescein. *Pflugers Arch* 1976; **364**: 83–89.
9. Pietruck F, Ullrich KJ. Transport interactions of different organic cations during their excretion by the intact rat kidney. *Kidney Int* 1995; **47**: 1647–1657.
10. Stachon A, Schlatter E, Hohage H. Dynamic monitoring of organic cation transport processes by fluorescence measurements in LLC-PK1 cells. *Cell Physiol Biochem* 1996; **6**: 72–81.
11. Stachon A, Hohage H, Feidt C *et al*. Characterisation of organic cation transport across the apical membrane of proximal tubular cells with the fluorescent dye 4-Di-1-ASP. *Cell Physiol Biochem* 1997; **7**: 264–274.
12. Hohage H, Stachon A, Feidt C *et al*. Regulation of organic cation transport in IHKE-1 and LLC-PK1 cells. Fluorometric studies with 4-(4-dimethylaminostyryl)-*N*-methylpyridinium. *J Pharmacol Exp Ther* 1998; **286**: 305–310.
13. Mehrens T, Lelleck S, Cetinkaya I *et al*. The affinity of the organic cation transporter rOCT1 is increased by protein kinase C-dependent phosphorylation. *J Am Soc Nephrol* 2000; **11**: 1216–1224.
14. Pietig G, Mehrens T, Hirsch JR *et al*. Properties and regulation of organic cation transport in freshly isolated human proximal tubules. *J Biol Chem* 2001; **276**: 33741–33746.
15. Pietruck F, Horbelt M, Feldkamp T *et al*. Digital fluorescence imaging of organic cation transport in freshly isolated rat proximal tubules. *Drug Metab Dispos* 2006; **34**: 339–342.
16. Montrose-Rafizadeh C, Mingard F, Murer H *et al*. Carrier-mediated transport of tetraethylammonium across rabbit renal basolateral membrane. *Am J Physiol* 1989; **257**: F243–F251.
17. Miyamoto Y, Tiruppathi C, Ganapathy V *et al*. Multiple transport systems for organic cations in renal brush-border membrane vesicles. *Am J Physiol* 1989; **256**: F540–F548.
18. Saito H, Yamamoto M, Inui K *et al*. Transcellular transport of organic cation across monolayers of kidney epithelial cell line LLC-PK. *Am J Physiol* 1992; **262**: C59–C66.
19. Urakami Y, Okuda M, Masuda S *et al*. Functional characteristics and membrane localization of rat multispecific organic cation transporters, OCT1 and OCT2, mediating tubular secretion of cationic drugs. *J Pharmacol Exp Ther* 1998; **287**: 800–805.
20. Gstraunthaler G, Seppi T, Pfaller W. Impact of culture conditions, culture media volumes, and glucose content on metabolic properties of renal epithelial cell cultures. Are renal cells in tissue culture hypoxic? *Cell Physiol Biochem* 1999; **9**: 150–172.
21. Lieberthal W, Nigam SK. Acute renal failure. II. Experimental models of acute renal failure: imperfect but indispensable. *Am J Physiol Renal Physiol* 2000; **278**: F1–F12.
22. Ullrich KJ, Papavassiliou F, David C *et al*. Contraluminal transport of organic cations in the proximal tubule of the rat kidney. I. Kinetics of *N*1-methylnicotinamide and tetraethylammonium, influence of K+, HCO3-, pH; inhibition by aliphatic primary, secondary and tertiary amines and mono- and bisquaternary compounds. *Pflugers Arch* 1991; **419**: 84–92.
23. David C, Rumrich G, Ullrich KJ. Luminal transport system for H+/organic cations in the rat proximal tubule. Kinetics, dependence on pH: specificity as compared with the contraluminal organic cation-transport system. *Pflugers Arch* 1995; **430**: 477–492.
24. Dunn KW, Sandoval RM, Kelly KJ *et al*. Functional studies of the kidney of living animals using multicolor two-photon microscopy. *Am J Physiol Cell Physiol* 2002; **283**: C905–C916.
25. Sutton TA, Mang HE, Campos SB *et al*. Injury of the renal microvascular endothelium alters barrier function after ischemia. *Am J Physiol Renal Physiol* 2003; **285**: F191–F198.
26. Yu W, Sandoval RM, Molitoris BA. Quantitative intravital microscopy using a generalized polarity concept for kidney studies. *Am J Physiol Cell Physiol* 2005; **289**: C1197–C1208.
27. Tanner GA, Sandoval RM, Dunn KW. Two-photon *in vivo* microscopy of sulfonefluorescein secretion in normal and cystic rat kidneys. *Am J Physiol Renal Physiol* 2004; **286**: F152–F160.

28. Sutton TA, Horbelt M, Sandoval RM. Imaging vascular pathology. *Nephron Physiol* 2006; **103**: p82–p85.

29. Helmchen F, Denk W. Deep tissue two-photon microscopy. *Nat Methods* 2005; **2**: 932–940.

30. Fluhler E, Burnham VG, Loew LM. Spectra, membrane binding, and potentiometric responses of new charge shift probes. *Biochemistry* 1985; **24**: 5749–5755.

31. Clarke RJ. Effect of lipid structure on the dipole potential of phosphatidylcholine bilayers. *Biochim Biophys Acta* 1997; **1327**: 269–278.

32. Schäli C, Schild L, Overney J *et al.* Secretion of tetraethylammonium by proximal tubules of rabbit kidneys. *Am J Physiol* 1983; **245**: F238–F246.

33. Dantzler WH, Brokl OH, Wright SH. Brush-border TEA transport in intact proximal tubules and isolated membrane vesicles. *Am J Physiol* 1989; **256**: F290–F297.

34. Dantzler WH, Brokl OH. N1-methylnicotinamide transport by isolated perfused snake proximal renal tubules. *Am J Physiol* 1986; **250**: F407–F418.

35. Goralski KB, Sitar DS. Tetraethylammonium and amantadine identify distinct organic cation transporters in rat renal cortical proximal and distal tubules. *J Pharmacol Exp Ther* 1999; **290**: 295–302.

36. Urakami Y, Okuda M, Masuda S *et al.* Distinct characteristics of organic cation transporters, OCT1 and OCT2, in the basolateral membrane of renal tubules. *Pharm Res* 2001; **18**: 1528–1534.

37. Pritchard JB, Sykes DB, Walden R *et al.* ATP-dependent transport of tetraethylammonium by endosomes isolated from rat renal cortex. *Am J Physiol* 1994; **266**: F966–F976.

38. Mewes HW, Rafael J. The 2-(dimethylaminostyryl)-1-methylpyridinium cation as indicator of the mitochondrial membrane potential. *FEBS Lett* 1981; **131**: 7–10.

39. Turkewitsch P, Darling GD, Powell WS. Enhanced fluorescence of 4-(*p*-dimethylaminostyryl)pyridinium salts in the presence of biological macromolecules. *J Chem Soc* 1998; **94**: 2083–2087.

40. Molitoris BA, Sandoval R, Sutton TA. Endothelial injury and dysfunction in ischemic acute renal failure. *Crit Care Med* 2002; **30**: S235–S240.

41. Berchner-Pfannschmidt U, Wotzlaw C, Merten E *et al.* Visualization of the three-dimensional organization of hypoxia-inducible factor-1 alpha and interacting cofactors in subnuclear structures. *Biol Chem* 2004; **385**: 231–237.